Redox Dependent Changes at the Heme Propionates in Cytochrome *c* Oxidase from *Paracoccus denitrificans*: Direct Evidence from FTIR Difference Spectroscopy in Combination with Heme Propionate ^{13}C Labeling†

Julia Behr,‡ Petra Hellwig,‖ Werner Mäntele,‖ and Hartmut Michel*,‡

Max-Planck-Institut für Biophysik, Abteilung Molekulare Membranbiologie, Heinrich-Hoffmann-Strasse 7, D-60528 Frankfurt/Main, Germany, and Institut für Biophysik, Theodor-Stern-Kai 7, Haus 74, D-60590 Frankfurt/Main, Germany

Received December 29, 1997; Revised Manuscript Received March 16, 1998

ABSTRACT: Specific isotope labeling at the carboxyl groups of the four heme propionates of cytochrome *c* oxidase from *Paracoccus denitrificans* was used in order to assign signals observed in electrochemically induced redox Fourier transform infrared (FTIR) difference spectra of this enzyme. For this purpose, the *hemA* gene of the *P. denitrificans* strain PD1222, coding for 5-aminolevulinate synthase, was deleted by partial replacement with a kanamycin resistance cartridge, resulting in a stable 5-aminolevulinic acid (ALA) auxotrophy. Normal growth of this deficient strain and cytochrome *c* oxidase yield comparable to that of *P. dentrificans* wild-type strain PD1222 could be obtained by supplementation with 0.1 mM ALA in the growth medium. Visible spectra and reduced-minus-oxidized FTIR spectra showed that the purified cytochrome *c* oxidase had spectral characteristics identical to those of the wild-type enzyme. The decrease of a negative signal at 1676 cm^{-1} in the reduced-minus-oxidized FTIR difference spectra of the ^{13}C-labeled cytochrome *c* oxidase in comparison to those of the unlabeled protein allowed the assignment of this signal to a COOH vibration mode of at least one of the four heme propionates. Moreover, a negative band at approximately 1570 cm^{-1} shifted to smaller wavenumbers in the spectra of the ^{13}C-labeled enzyme in comparison to the spectra of the unlabeled enzyme and was thus assigned to contributions from an antisymmetric COO^- mode of one or more of the four heme propionates. Additionally, a positive signal at 1538 cm^{-1} shifted to approximately 1500 cm^{-1} in the spectra of the isotopically labeled protein and was therefore assigned to at least one antisymmetric COO^- mode of the heme propionates. A negative signal at 1390 cm^{-1}, which has been shifted to 1360 cm^{-1} in the spectra of the ^{13}C-labeled enzyme, is due to a symmetric COO^- mode from at least one heme propionate. These results suggest that at least two of the four heme propionates in cytochrome *c* oxidase undergo significant vibrational changes upon reduction of the enzyme, either by protonation/deprotonation or by environmental changes.

Cytochrome *c* oxidase is the terminal enzyme of the respiratory chain in mitochondria and many bacteria and catalyzes the reduction of oxygen to water. In this process, the electron transfer from cytochrome *c* to oxygen and water formation are efficiently coupled to the formation of an electrochemical proton gradient that drives ATP synthesis. Several mutagenetic and spectroscopic approaches have provided insight into mechanistic details of the catalytic process and the linkage of oxygen reduction and proton pumping (for review, see refs *1* and *2*). Recently the structures of the four subunits containing cytochrome *c* oxidase from *P. denitrificans* (*3*) and of the 13 subunits containing enzyme from bovine heart mitochondria (*4, 5*) have been determined by X-ray crystallography. Four redox-active sites are involved in the electron transfer. The binuclear Cu_A center bound to subunit II is the first electron acceptor from cytochrome *c*. Then electrons are transferred via heme *a*, localized in subunit I, to the binuclear center consisting of Cu_B and heme a_3, which are also bound to subunit I and where the oxygen reduction takes place. Protons are involved in cytochrome *c* oxidase catalysis for two different functions: "chemical" protons must be available to the binuclear center in order to form water. Additionally, "pumped" protons are translocated across the membrane adding to the generation of the proton gradient. Both chemical and pumped protons are taken up from the cytoplasmic side. For proton transfer, two separate pathways have been indicated on the basis of the X-ray structure of the *P. denitrificans* enzyme and from site-directed mutants in which proton translocation was affected (*6*−*8*). Iwata et al. (*3*) originally predicted a pathway from residue Asp 124 to Glu 278 in subunit I as the one for the pumped protons since an Asp 124 to Asn mutant cytochrome *c* oxidase is inactive with respect to proton pumping but still retains some capability for enzymatic turnover. This pathway is less

† Financial support was provided by Deutsche Forschungsgemeinschaft via Sonderforschungbereich, the Fonds der Chemischen Industrie, and the Max-Planck-Gesellschaft.

* To whom correspondence should be addressed. E-mail: michel@mpibp-frankfurt.mpg.de; telephone: 49 69 96769 401; fax: 49 69 96769 423.

‡ Max-Planck-Institut für Biophysik.

‖ Institut für Biophysik.

S0006-2960(97)03169-3 CCC: $15.00
Published on Web 04/30/1998

clearly defined beyond the residue Glu 278 in subunit I. Two possibilities have been suggested. First, Pro 277 and bound water molecules might be involved in proton transfer to the binuclear center. Alternatively, a direct route from Glu 278 to one of the heme a_3 propionates might be possible, because these side chains could approach one another to hydrogen-bonding distance through conformational changes (*3, 9*).

The mechanism of coupling the redox chemistry to proton pumping is of particular interest. A recent suggestion is the histidine cycle mechanism (*10*) where the side chain of a histidine ligand of Cu_B cycles twice between imidazolate, imidazole, and imidazolium states. This histidine is proposed to be in the imidazolate state in the oxidized enzyme and is converted to the imidazolium state upon reduction of the enzyme. A similar, but more general "proton trap" model (*11*) states that the protons that are taken up upon reduction of the binuclear center in order to maintain electroneutrality are expelled later by the protons required for water formation during the reaction cycle. An uptake of about two protons upon reduction of the binuclear center and of about 0.5 proton upon reduction of heme *a* has been observed experimentally (*11*−*13*). For an experimental verification of the pumping mechanism, the identification of the protons accepting side chains or groups is crucial. The heme propionates are possible candidates for becoming protonated upon reduction.

The possible functions of individual amino acid side chains as proton traps or their participation in the proton pathway can be investigated by site-directed mutagenesis. In the case of the propionates, a different approach had to be selected. In this work, we have studied the possible role of the heme propionates in redox reactions using a combination of isotopic labeling and redox-FTIR[1] difference spectroscopy. As previously reported (*14*) electrochemically induced reduced-minus-oxidized FTIR difference spectra reflect rearrangements concomitant with the redox reactions of the enzyme and yield information about the involvement of specific groups in processes that are coupled to the redox reactions. As mentioned in an earlier work (*14*), the C═O stretching modes of protonated heme propionates are expected to appear in the spectral range from 1700 to 1665 cm^{-1}. Contributions from antisymmetric and symmetric COO^- stretching modes of the corresponding deprotonated carboxyl groups can be localized at approximately 1620−1540 cm^{-1} and 1420−1300 cm^{-1}, respectively. To conclusively assign the observed signals in these regions, the four heme propionates were $^{13}COOH$ labeled thus causing a downshift of corresponding bands to smaller wavenumbers.

For this purpose, it was necessary to develop a method for the preparation of isotopically labeled cytochrome *c* oxidase, which guarantees a very efficient and specific ^{13}C enrichment at the carboxyl groups of the heme propionates. Previously, Rivera and Walker (*15*) described a method for the preparation of isotopically enriched heme. They utilized the efficient heterologous expression of the heme binding protein cytochrome b_5 from rat together with an enhanced biosynthesis of heme induced by addition of the heme precursor ALA to the bacterial host *Escherichia coli*. In this way, they obtained an isotope enrichment of more than 85%. For the labeling of the cytochrome *c* oxidase from *P. denitrificans*, we have constructed a *P. denitrificans* strain that is deficient in heme synthesis. Upon supplementing this deletion strain with a ^{13}C-labeled heme precursor, complete labeling can be expected. In this case, the isotopic enrichment at the heme propionates is only limited by the isotopic enrichment of the used heme precursor, which was almost 100% in our case.

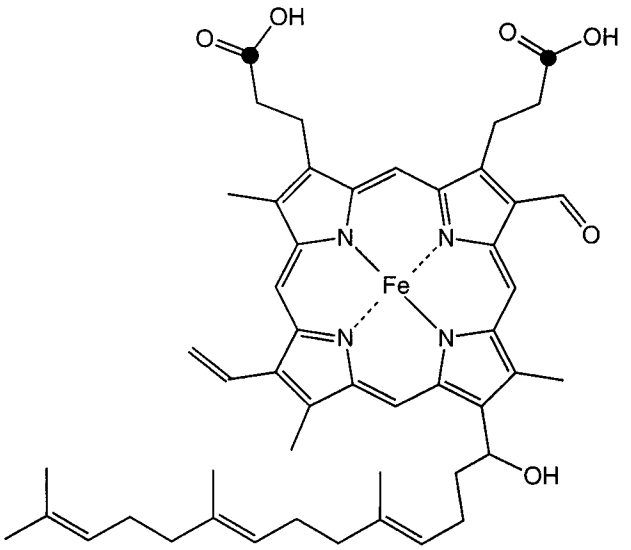

FIGURE 1: Schematic representation of heme A, ^{13}C-isotopically labeled at the carboxyl groups of the heme propionates after supplementation with [1-^{13}C]-5-aminolevulinic acid as a heme precursor. The two carbon atoms labeled are marked ●.

The first committed precursor in the biosynthetic pathway of heme is ALA. Two different routes for ALA biosynthesis are found in nature. The so-called Shemin pathway utilizes the one-step condensation of glycine and succinyl-coenzyme A by ALA synthase and is found in the α-group of the proteobacteria, in yeast, and in mammalian cells (*16*−*18*). *P. denitrificans* as well as *Rhodobacter sphaeroides*, belonging to this α-group of the proteobacteria, exclusively use this pathway for ALA synthesis. In contrast to *R. sphaeroides*, which has two gene loci for the ALA synthase (*hemA* and *hemT*; *19*), *P. denitrificans* and *R. capsulatus* possess only one gene locus (*hemA*; *20, 21*). For the construction of the deficient mutant, it was therefore sufficient to disrupt the *hemA* gene of *P. denitrificans* resulting in an ALA auxotrophy (*21*). If [1-^{13}C]-5-aminolevulinate is now used as a heme precursor, the heme propionates of both hemes are labeled at the carboxyl groups, with no ^{13}C enrichment at any other site as shown in Figure 1.

EXPERIMENTAL PROCEDURES

Media and Growth Conditions. *P. denitrificans* strain PD1222 (*22*) was grown aerobically on succinate medium (*23*) at 32 °C and harvested at late exponential phase. The deficient *P. denitrificans* strain was additionally supplemented with 0.1 mM 5-aminolevulinate dihydrochloride. *E. coli* strains were grown in LB (Luria−Bertani medium) at 37 °C. Antibiotics were added in the following concentrations (in micrograms per milliliter): *E. coli*, ampicillin (100), kanamycin (50), streptomycin (25); *P. denitrificans*, kanamycin (100), spectinomycin (50), and rifampicin (60).

[1] Abbreviations: ALA, 5-aminolevulinic acid; bp, base pairs; FTIR, Fourier transform infrared; IR, infrared; kbp, kilo base pairs; LB, Luria−Bertani medium; OD, optical density; PCR, polymerase chain reaction; SHE, standard hydrogen electrode; VIS, visible.

^{13}C-labeled ALA was supplemented in growth medium in order to obtain the ^{13}C-labeled hemes incorporated into cytochrome *c* oxidase. The following procedure has been employed using unlabeled ALA for control experiments and using [1-^{13}C]-5-aminolevulinic acid for the specific labeling.

The deletion mutant DAS1 grown on a plate was used to inoculate 30 mL of succinate medium supplemented with kanamycin, spectinomycin, and 0.1 mM unlabeled or [1-^{13}C]-5-aminolevulinic acid and was allowed to grow until the OD_{650} (optical density, measured with a LKB Ultrospec Plus spectrophotometer, Pharmacia, Freiburg, FRG) was 4.0 (approximately 12 h). This culture was used to inoculate 1 L of succinate medium also containing kanamycin, spectinomycin, and 0.1 mM unlabeled or [1-^{13}C]-5-aminolevulinic acid. After growth to $OD_{650} = 3.0$, 50 mL of this culture was used to inoculate 2 L of succinate medium containing kanamycin and 0.1 mM unlabeled or [1-^{13}C]-5-aminolevulinic acid, respectively. The cells were harvested at $OD_{650} = 3.0$.

Materials. All restriction endonucleases and nucleic acid-modifying enzymes were obtained from Gibco BRL (Eggenstein, FRG) or New England Biolabs (Beverly, MA). All antibiotics were purchased from Sigma (München, FRG). *N*-Dodecyl-β-D-maltoside was obtained from Calbiochem (Bad Soden/ Ts., FRG).

5-Aminolevulinate dihydrochloride was purchased from Merck (Darmstadt, FRG) whereas [1-^{13}C]-5-aminolevulinate dihydrochloride was obtained from Campro Scientific (Emmerich, FRG). All other chemicals were of analytical grade and were purchased from local distributors.

DNA Isolation and Manipulation. Isolation of DNA and standard recombination DNA techniques were performed according to Sambrook et al. (*24*), if not indicated otherwise.

Southern blot analysis was performed with chromosomal DNA transferred to a nylon membrane (Biodyne A, PALL, Portsmouth, U.K.) by capillary forces. For labeling of probes and detection of DNA, the nonradioactive DNA labeling and detection kit from Boehringer-Mannheim (Mannheim, FRG) was used.

Published methods were applied for the triparental mating procedure involving the *E. coli* strain MM294 (*25*). The suicide vector pRVS1 (*26*) was used for the construction of the deficient strain.

Isolation, Purification, and Steady-State Kinetics of Cytochrome c Oxidase. Membranes were prepared as described (*27*) and solubilized with the detergent *N*-dodecyl-β-D-maltoside (*28*). The protein was purified by streptavidin affinity chromatography (*28*). An engineered monoclonal antibody fragment (Fv) linked to the strep tag and directed against an epitope on the periplasmic domain of the subunit II was used for affinity purification of a cytochrome *c* oxidase−Fv complex (*29*). Excess antibody fragment was removed by HPLC gel filtration (*29*). Steady-state kinetic measurements with reduced horse heart cytochrome *c* were carried out as described by Witt et al. (*30*).

For spectroelectrochemistry, the detergent was exchanged to 3.2 mM *N*-decyl-β-D-maltoside, and the buffer was replaced by 200 mM phosphate buffer, pH 7.0, containing 100 mM KCl by repeated dilution and concentration of the sample in the desired buffer. The sample was concentrated to a protein concentration of approximately 0.5−1 mM using Microcon ultrafiltration cells (Amicon, Witten, FRG).

Electrochemistry. The spectroelectrochemical cell for the VIS and IR range was used as described previously (*31*−*33*). With a path length of 6−10 μm, a sufficient transmission for the spectral range from 2000 to 1000 cm^{-1}, even for the strong water absorption at 1650 cm^{-1}, was achieved. The gold grid working electrode was chemically modified in a 2 mM cysteamine solution for 1 h and then carefully washed with deionized water. To accelerate the redox reactions, mediators were added as described by Baymann (*32*). FTIR signals from the mediators are only observed in the spectral range from 1200 to 1000 cm^{-1} due to proton uptake/release (see Results and Discussion). Potentials quoted with the data refer to the Ag/AgCl/3 M KCl reference electrode (add +208 mV for SHE potentials).

Spectroscopy. FTIR and VIS difference spectra as a function of the applied potential were obtained simultaneously combining an IR (4000−1000 cm^{-1}) and a VIS beam (400−900 nm) as previously described (*34*). For difference spectra, the samples were equilibrated at an initial potential at the electrode, and single beam spectra in the VIS and the IR range were recorded as references. After equilibrating the samples at the final potential, further single beam spectra were recorded. Difference spectra as presented in this work were calculated from these two single beam spectra, with the initial single beam spectrum taken as reference. This procedure results in FTIR difference spectra with negative bands for the initial state and positive bands for the final state. The equilibration process was followed by monitoring the electrode current and by successively recording spectra in the VIS and IR range until no further changes could be observed and full equilibration was reached. For the full potential step from 0.5 to −0.5 V, equilibration time was about 5 min. Typically 128 interferogramms at 4 cm^{-1} resolution were co-added for each single beam spectrum and transformed using triangular apodization. To improve the signal-to-noise ratio, five difference spectra were averaged. No smoothing or deconvolution procedures were applied.

RESULTS AND DISCUSSION

Construction of the ALA-Synthase Deletion Strain of P. denitrificans. The 1.26 kbp ALA-synthase gene *hemA* was obtained by PCR using genomic DNA of *P. denitrificans* as a template and was subcloned in pUC 18 (*35*) using *Xba*I/*Bam*HI restriction sites that are located in the PCR primers used. After replacing a 220 bp *Xcm*I/*Bst*XI restriction endonuclease fragment with a 1.8 kbp kanamycin resistance cartridge, this recombination cartridge (converted to blunt ends) was cloned into the *Sma*I site of the broad host range vector pRVS1 (*26*). The plasmid obtained (pRAS) was transferred to *P. denitrificans* via conjugation. The resulting plasmid integrant strains were selected in the presence of kanamycin (300 mg/L). In addition, 0.1 mM ALA was added to all media because the disruption of the *hemA* gene in *P. denitrificans* resulted in an ALA auxotrophy (*21*).

Single crossover recombinants could be observed as blue colonies on plates supplemented with 5-bromo-4-chloro-3-indolyl-β-D-galactoside (X-Gal, 20 μg/mL) whereas double crossover recombinants remained white (*26*). The double and single crossover recombinants were obtained in a ratio of 1:10.

Southern blot analysis of the genomic DNA of the ALA-synthase deficient mutant strain DAS1 confirmed that the

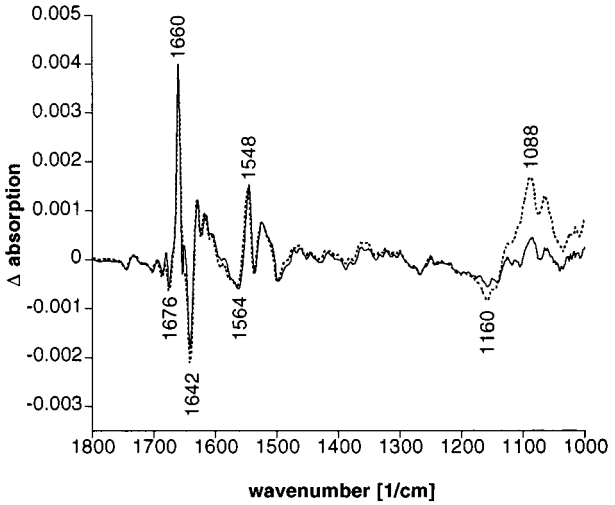

FIGURE 2: Reduced-minus-oxidized FTIR difference spectra of the wild-type enzyme (solid line) and the unlabeled cytochrome *c* oxidase from the deficient strain (dashed line) obtained for a potential step from 0.5 to −0.5 V (vs Ag/AgCl/3 M KCl). Conditions: approximately 0.5 mM cytochrome *c* oxidase in 200 mM phosphate buffer, pH 7, with 100 mM KCl as electrolyte and mediators as described.

ALA-synthase gene was interrupted by the kanamycin resistance cartridge (data not shown). Digestion with *Eco*RI endonuclease and subsequent hybridization of the nonradioactively labeled *hemA* gene proved the integration of the 1.8 kbp kanamycin resistance gene as well as the absence of the 220 bp *Xcm*I/*Bst*XI fragment. The procedure resulted in two *Eco*RI restriction fragments of approximately 2.0 and 2.6 kbp using the wild-type gene probe and only one *Eco*RI restriction fragment of 6.2 kbp using the deficient mutant probe. The latter result is due to the removal of the *Xcm*I/*Bst*XI fragment,which bears an *Eco*RI restriction site, and the addition of the 1.8 kbp kanamycin resistance gene. The stability of the deficient mutant could be easily checked by ALA auxotrophy at any time.

Characterization of the Cytochrome c Oxidase Isolated from the Deficient Strain. After supplementation of the deficient strain with 0.1 mM unlabeled ALA, normal growth was restored and cytochrome *c* oxidase could be purified with a yield comparable to that of the wild-type strain PD1222. Enzymatic turnover of the purified enzyme determined by oxidation of reduced horse heart cytochrome *c* was also identical to that of the wild-type enzyme.

Visible spectra of oxidized and reduced cytochrome *c* oxidase from the deficient strain were indistinguishable from those of the wild-type enzyme. This clearly demonstrates that the oxidase obtained from the deficient strain supplemented with 0.1 mM ALA has the same heme *a* to heme a_3 ratio as the wild-type enzyme. In a further control experiment, the reduced-minus-oxidized FTIR difference spectra of cytochrome *c* oxidase from the wild type (solid line) and from the deficient strain (dashed line) are compared for the full potential step from 0.5 to −0.5 V (Figure 2). Because of slightly different sample concentrations, the spectra were normalized for the α-band signal in the reduced-minus-oxidized visible spectrum simultaneously measured. The reduced-minus-oxidized FTIR difference spectrum of the wild-type enzyme has already been presented and described in previous work (*14*). The changes induced by the electrochemical redox reaction have been shown to be fully reversible (*14*). The reduced-minus-oxidized spectrum and the oxidized-minus-reduced spectrum are exact mirror images. This reversibility is even evident for minute bands. No data smoothing, baseline correction, or deconvolution procedures were applied. The noise level can be estimated either at frequencies above 1780 cm^{-1}, where no signal appears as well as by blank difference spectra calculated from two single beam spectra recorded at the same electrode potential or after a potential cycle (−0.5 to 0.5 V followed by 0.5 to −0.5 V). The noise level is estimated to be around $25-50 \times 10^{-6}$ absorbance units. Only in regions of strong absorbance of the sample, such as around 1650 cm^{-1} (water OH modes and amide I modes), the noise level is slightly higher. As described (*14*), the small amplitude of the prominent signals in the range of the amide I mode absorbance from the polypeptide backbone (predominantly a C═O vibration mode between 1680 and 1620 cm^{-1}) precludes sizable conformational changes of the protein, thus the redox reaction seems to affect only a few amide modes. The spectrum of the cytochrome *c* oxidase from the deficient strain is essentially identical to that of the wild-type enzyme. Minor differences in the region of the water band absorption at 1650 cm^{-1} can be explained by the higher noise level in this spectral range because of strong background absorbance. Additionally, the strong bands in the spectral range from 1200 to 1000 cm^{-1} differ in the two spectra. In this region, the broad difference signals at 1088 and 1160 cm^{-1} dominate, which were previously assigned by us to PO modes from phosphate buffer indicating proton uptake or release of the enzyme and the mediators in the course of the redox reaction (*14*). These bands may also vary in different spectra of the wild-type enzyme.

Apart from these signals, no differences between the spectra of the enzyme from the deficient strain and that from the wild type were observed. Thus, supplementation of the growth medium with ALA restores completely normal cytochrome *c* oxidase synthesis, and the purified protein has spectral characteristics identical to those of the wild-type protein.

Comparison of the Reduced-Minus-Oxidized FTIR Difference Spectra of Unlabeled and Specifically Labeled Cytochrome c Oxidase. The reduced-minus-oxidized FTIR difference spectra of the unlabeled (dashed line) and the specifically ^{13}C-labeled cytochrome *c* oxidase (solid line) for the potential step from 0.5 to −0.5 V are shown in Figure 3. Four signals have been identified that shift upon isotopic labeling of the heme propionates. Thus, they can exclusively be assigned to vibrational modes of the heme propionates. Although it cannot be excluded that more than one propionate is involved in one shifted signal, we will use the singular form in the following.

The spectral range from 1700 to 1670 cm^{-1}, shown expanded in Figure 4, indicates clear changes in the band patterns upon labeling. As mentioned above, the C═O stretching vibrations of heme propionate COOH groups are expected to appear in this spectral region. The amplitude of the negative signal at 1676 cm^{-1} decreased significantly in the spectrum of the specifically ^{13}C-labeled protein (solid line) as compared to that of the unlabeled enzyme (dashed line). Alterations at this spectral position have to be treated carefully, since the signal at 1676 cm^{-1} is still within the

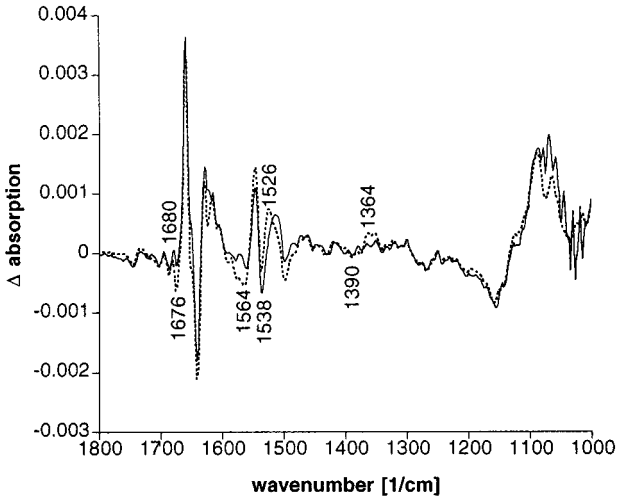

FIGURE 3: Comparison of the reduced-minus-oxidized FTIR difference spectra of the unlabeled (dashed line) and the ^{13}C-labeled cytochrome *c* oxidase (solid line) obtained for a potential step from 0.5 to −0.5 V. Conditions as in Figure 2.

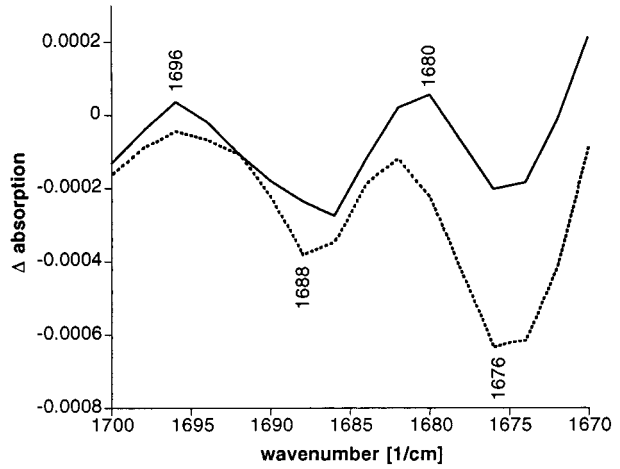

FIGURE 4: The 1700−1670 cm^{-1} region of the reduced-minus-oxidized FTIR difference spectra of the unlabeled (dashed line) and the ^{13}C-labeled cytochrome *c* oxidase (solid line) obtained for a potential step from 0.5 to −0.5 V.

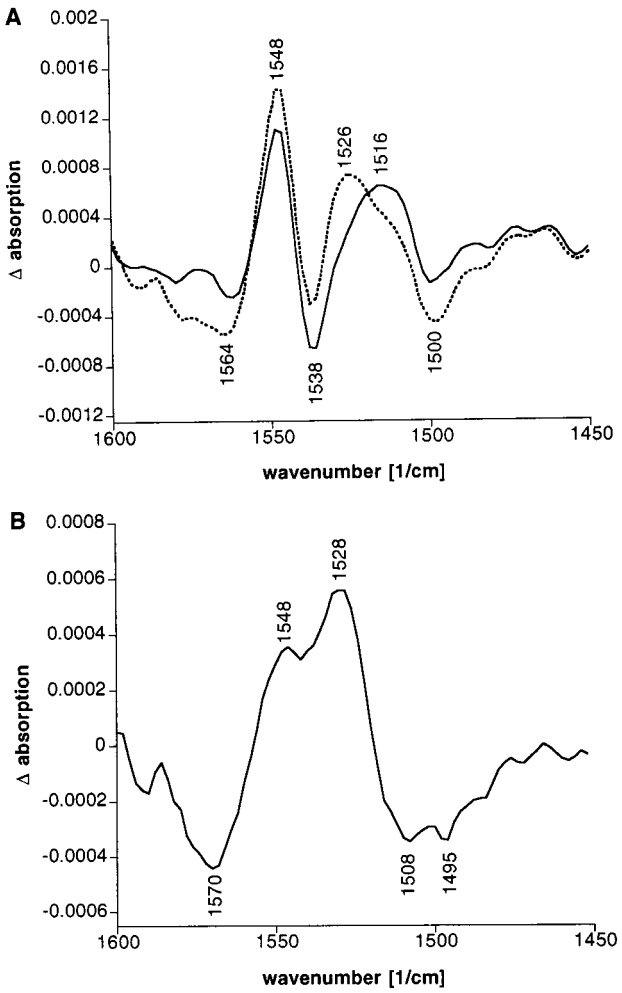

FIGURE 5: (A) The 1600−1450 cm^{-1} region of the reduced-minus-oxidized FTIR difference spectra of the unlabeled (dashed line) and the ^{13}C-labeled cytochrome *c* oxidase (solid line) obtained for a potential step from 0.5 to −0.5 V. (B) The double difference spectrum obtained by subtracting the spectrum of the ^{13}C-labeled protein from that of the unlabeled enzyme for the spectral region from 1600 to 1450 cm^{-1}.

expected range of the very strong amide I mode absorbance from the polypeptide backbone, which usually appears in the 1680−1620 cm^{-1} region. Furthermore, the signal is close to the broad water band absorption at 1650 cm^{-1}. Thus the noise level in this spectral range is slightly higher than in the rest of the spectrum (apart from the region between 1200 and 1000 cm^{-1}, see above). Nevertheless, the observed decrease of the negative signal at 1676 cm^{-1} upon this specific $^{12}C/^{13}C$ exchange is a reproducible feature. This result allows an assignment of part of this negative signal to a COOH mode of a heme propionate. In a simple reduced-mass calculation assuming a localized C═O band, a downshift of ∼38 cm^{-1} from $^{12}COOH$ to $^{13}COOH$ would be expected. Thus the signal is expected to shift even more into the amide I region, approximately to 1638 cm^{-1}. However, minor differences in this region could also be due to a higher noise level in the range of the water band absorption as mentioned above. Previous work with ^{13}C-labeled compounds indicates that the isotope shift might well be smaller, assuming coupling of the C═O group to the rest of the molecule. It is not possible to precisely predict the position of the shifted signal. We consider its shift to the amide I region as likely, where it is obscured by other, much stronger signals.

The negative signal at 1676 cm^{-1} did not disappear completely upon $^{12}C/^{13}C$ exchange, indicating that this difference band is composed of several components. In addition to the COOH mode of the heme propionate, amide I C═O modes might also contribute to the signal.

In the highly reproducible region from 1600 to 1450 cm^{-1} that is shown expanded in Figure 5A, very strong changes can be observed upon labeling. In the region between 1560 and 1520 cm^{-1}, coupled CN stretching and NH bending modes from the protein backbone (amid II modes) are predicted to appear. As reported in a previous publication (*14*), an assignment of all signals in this region to these amide II modes is not possible since the bands do not show the expected strong shifts upon H/D exchange (data not shown). Signals from the antisymmetric COO^- stretching modes might appear in addition to possible contributions from heme C═C groups. To demonstrate the changes that occur in this spectral range upon $^{12}C/^{13}C$ exchange, a double difference spectrum of both reduced-minus-oxidized FTIR difference spectra has been calculated by subtracting the spectrum of

the ^{13}C-labeled protein from that of the unlabeled enzyme. The region from 1600 to 1450 cm^{-1} of the double difference spectrum obtained is shown in Figure 5B. This spectrum clearly demonstrates that a negative band at approximately 1570 cm^{-1} has been shifted to the area between 1548 and 1528 cm^{-1} (to approximately 1538 cm^{-1}) in the spectrum of the ^{13}C-labeled enzyme, indicating a shift of about ~32 cm^{-1} to smaller wavenumbers. Additionally, a positive band has been shifted from approximately 1538 cm^{-1} to about 1500 cm^{-1} upon $^{12}C/^{13}C$ exchange. Thus these two signals are strongly suggested to arise from antisymmetric COO^- stretching modes of the heme propionates. For this spectral region, a downshift of ~38−40 cm^{-1} from $^{12}COO^-$ to $^{13}COO^-$ would be estimated from reduced-mass calculations (*36*). Both observed spectral shifts are within the predicted order, considering that the isotope shift might well be smaller than the calculated value.

These results indicate that a COO^- mode of one heme propionate disappears whereas a COO^- mode of one heme propionate appears upon reduction of the cytochrome *c* oxidase.

Small changes of the band intensities occur in the spectral range from 1420 to 1310 cm^{-1} upon $^{12}C/^{13}C$ exchange, where symmetric stretching vibrations of COO^- groups are expected. If signals in this range belonged to the heme propionates, a downshift of ~35 cm^{-1} from $^{12}COO^-$ to $^{13}COO^-$ would be predicted (*36*). This region is shown expanded in Figure 6A; the double difference spectrum for the same spectral range is shown in Figure 6B.

Figure 6B clearly exhibits a shift of the negative signal at approximately 1390 cm^{-1} in the reduced-minus-oxidized FTIR difference spectrum to a signal at about 1360 cm^{-1} upon isotopic labeling. We thus suggest that part of the negative signals near 1390 cm^{-1} in the spectrum of the unlabeled protein is due to a symmetric COO^- vibrational mode of a heme propionate. The COO^- group could be identical to that contributing to the negative signal at approximately 1570 cm^{-1} by its corresponding antisymmetric stretching vibration. For the antisymmetric COO^- mode at about 1538 cm^{-1}, no corresponding symmetric vibrational mode could be identified in this region.

For the interpretation of a signal in the reduced-minus-oxidized FTIR spectrum being assigned to the carboxyl group of a heme propionate, two scenarios are possible. The signal might be caused by conformational changes upon the reduction of the protein or by a protonation/deprotonation reaction of the heme propionate. Additionally, a combination of both might be possible. Thus the negative signal at 1676 cm^{-1} assigned to a COOH mode of a heme propionate in the reduced-minus-oxidized FTIR difference spectrum might be caused by a deprotonation reaction of a carboxyl group upon reduction of the protein. Changes in the environment of a protonated propionate or the movement of the propionate itself upon the reduction of the protein are also conceivable. In this case, one would generally expect an accompanied shift of a positive contribution in the spectral range of COOH modes upon $^{12}C/^{13}C$ exchange. Such a corresponding positive signal could be located in the amide I region where a band shift upon $^{12}C/^{13}C$ exchange might be undetectable. Alternatively, the environmental changes upon reduction of the protein might just affect the extinction coefficient of the signal at 1676 cm^{-1} whereas its frequency might remain

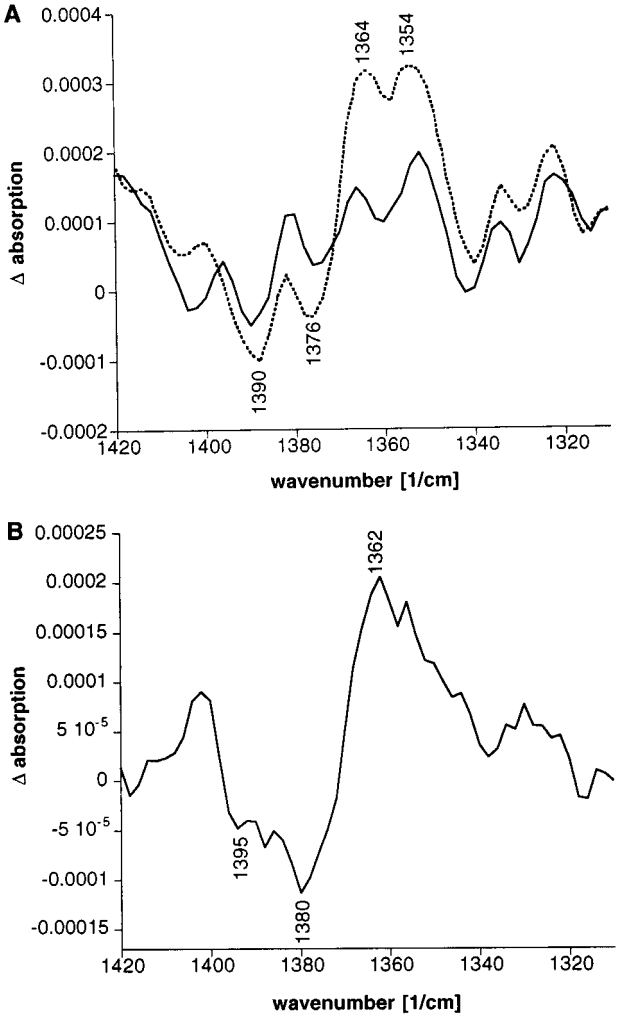

FIGURE 6: (A) The 1420−1310 cm^{-1} region of the reduced-minus-oxidized FTIR difference spectra of the unlabeled (dashed line) and the ^{13}C-labeled cytochrome *c* oxidase (solid line) obtained for a potential step from 0.5 to −0.5 V. (B) The double difference spectrum obtained by subtracting the spectrum of the ^{13}C-labeled protein from that of the unlabeled enzyme for the spectral region from 1420 to 1310 cm^{-1}.

unchanged, so that no corresponding positive signal would be obtained.

The observed disappearance of the antisymmetric and symmetric stretching vibration of a COO^- group (at approximately 1570 and 1390 cm^{-1}, respectively) and the simultaneous appearance of the antisymmetric stretching vibration of a COO^- group at 1538 cm^{-1} upon reduction of the cytochrome *c* oxidase could be due to protonation changes of different heme propionates, i.e., a protonation reaction in the first case and a deprotonation reaction in the latter case. The appearance of the COO^- mode at 1538 cm^{-1} might correspond directly to the disappearance of the COOH mode observed at 1676 cm^{-1} in the reduced-minus-oxidized FTIR difference spectrum, whereas for the disappearance of the COO^- mode at 1570 cm^{-1} no corresponding appearance of a COOH mode could be found. Again, such a mode might be obscured by other very strong signals and would not be evident in the comparison of the spectra of the unlabeled and the specifically labeled enzyme.

Additionally, a conformational change of a deprotonated heme propionate to an extremely different environment or strong changes in the direct environment of a deprotonated

heme propionate are conceivable, so that the same COO^- group might absorb at approximately 1570 cm^{-1} in the oxidized and at approximately 1538 cm^{-1} in the reduced state.

CONCLUSIONS

Specific isotopic labeling provides an excellent tool for redox-FTIR investigations and avoids structural changes that can arise upon site-directed mutagenesis work. A method for the preparation of isotopically labeled cytochrome *c* oxidase has been developed that guarantees a very efficient and specific ^{13}C-enrichment at the carboxyl groups of the heme propionates. The protein obtained from these preparations has spectral characteristics and cytochrome *c* oxidase activity identical to those of the wild type. The ^{13}C-labeled enzyme was then used to assign signals observed in the reduced-minus-oxidized FTIR difference spectrum of cytochrome *c* oxidase to COOH and COO^- vibration modes of the heme propionates. Upon electrochemical reduction of cytochrome *c* oxidase, the disappearance of at least one COOH mode and one or more COO^- mode(s) as well as the appearance of at least one COO^- mode of the heme propionates were observed. These results suggest that significant vibrational changes occur for at least two of the four heme propionates upon reduction of the enzyme. These changes might be due to protonation and deprotonation events upon the redox reaction or could be caused by environmental changes of protonated and deprotonated heme propionates, respectively. For the distinction between these possibilities, the assignment of the vibrational modes to specific heme propionates will be required. All four heme propionates are in strong interactions with several amino acids and parts of the protein backbone in the environment (*3*, *5*, *37*), so that the site-directed mutagenesis of the interacting amino acids should be accompanied with changes of the vibrational modes of the corresponding heme propionate. Thus, the spectroscopic analysis of these mutants will be a valuable tool for the assignment of the vibrational modes to specific heme propionates and thereby will help to elucidate the role of the specific heme propionates in the redox reaction of cytochrome *c* oxidase.

ACKNOWLEDGMENT

We are grateful to Hannelore Müller for technical assistance, and we thank Ingrid Albert, Axel Harrenga, Aimo Kannt, and Bernd Ludwig for valuable discussions and critical reading of the manuscript. We thank also Bernd Ludwig for providing the vector pRVS1 and the bacteria strains MM294 and Pd1222.

REFERENCES

1. Babcock, G. T., and Wikström, M. (1992) *Nature 356*, 301−309.
2. Ferguson-Miller, S., and Babcock, G. T. (1996) *Chem. Rev. 96*, 2889−2907.
3. Iwata, S., Ostermeier, C., Ludwig, B., and Michel, H. (1995) *Nature 376*, 660−669.
4. Tsukihara, T., Aoyama, H., Yamashita, E., Tomizaki, T., Yamaguchi, H., Shinzawa-Itoh, K., Nakashima, R., Yaono, R., and Yoshikawa, S. (1995) *Science 269*, 1069−1074.
5. Tsukihara, T., Aoyama, H., Yamashita, E., Tomizaki, T., Yamaguchi, H., Shinzawa-Itoh, K., Nakashima, R., Yaono, R., and Yoshikawa, S. (1996) *Science 272*, 1136−1144.
6. Thomas, J. W., Puustinen, A., Alben, J. O., Gennis, R. B., and Wikström, M. (1993) *Biochemistry 32*, 10923−10928.
7. Fetter, J. R., Quian, J., Shapleigh, J., Thomas, J. W., Garcia-Horsman, J. A., Schmidt, E., Hosler, J., Babcock, G. T., Gennis, R. B., and Ferguson-Miller, S. (1995) *Proc. Natl. Acad. Sci. U.S.A. 92*, 1604−1608.
8. Garcia-Horsman, J. A., Puustinen, A., Gennis, R. B., and Wikström, M. (1995) *Biochemistry 34*, 4428−4433.
9. Hofacker, I., and Schulten, K. (1998) *Proteins 30*, 100−107.
10. Morgan, J. E., Verkhovsky, M. I., and Wikström, M. (1994) *J. Bioenerg. Biomembr. 26*, 599−608.
11. Rich P. R. (1995) *Aust. J. Plant Physiol. 22*, 479−486.
12. Mitchell, R., and Rich, P. R. (1994) *Biochim. Biophys. Acta 1186*, 19−26.
13. Capitanio, N., Vygodina, T. V., Capitanio, C., Konstantinov, A. A., Nicholls, P., and Papa, S. (1997) *Biochim. Biophys. Acta 1318*, 255−265.
14. Hellwig, P., Rost, B., Kaiser, U., Ostermeier, C., Michel, H., and Mäntele, W. (1996) *FEBS Lett. 385*, 53−57.
15. Rivera, M., and Walker, F. A. (1995) *Anal. Biochem. 230*, 295−302.
16. Dailey, H. A. Ed., (1990) in *Biosynthesis of heme and chlorophylls*, McGraw-Hill, Hightstown, NJ.
17. Jordan, P. M. (1991) in *New comprehensive biochemistry* (Neuberger, A., and van Deenen, L. L. M., Eds.) Vol. 19, Elsevier, Amsterdam.
18. O'Neill, G. P., Jahn, D., and Söll, D. (1991) *Subcell. Biochem. 17*, 235−264.
19. Neidle, E. L., and Kaplan, S. (1993) *J. Bacteriol. 175*, 2292−2303.
20. Hornberger, U., Liebetanz, R., Tichy, H.-V., and Drews, G. (1990) *Mol. Gen. Genet. 221*, 371−378.
21. Page, M. D., and Ferguson, S. J. (1994) *J. Bacteriol. 176*, 5919−5928.
22. deVries, G. E., Harms, N., Hoogendijk, J., and Stouthamer, A. H. (1989) *Arch. Microbiol. 152*, 52−57.
23. Ludwig, B. (1986) *Methods Enzymol. 126*, 153−159.
24. Sambrook, J., Fritsch, E. F., and Maniatis, T. (1989) in *Molecular cloning: a laboratory manual*, 2nd ed., Cold Spring Harbor, Cold Spring Harbor, NY.
25. Simon, R. (1984) *Mol. Gen. Genet. 196*, 413−420.
26. Van Spanning, R. J. M., Wansell, C. W., Reijnders, W. N. M., Harms, N., Ras, J., Oltmann, L. F., and Stouthammer, A. H. (1991) *J. Bacteriol. 173*, 6962−6970.
27. Gerhus, E., Steinrücke, P., and Ludwig, B. (1990) *J. Bacteriol. 172*, 2392−2400.
28. Kleymann, G., Ostermeier, C., Ludwig, B., Skerra, A., and Michel, H. (1995) *Bio/Technology 13*, 155−160.
29. Ostermeier, C., Iwata, S., Ludwig, B., and Michel, H. (1995) *Nat. Struct. Biol. 2*, 842−846.
30. Witt, H., Zickermann, V., and Ludwig, B. (1995) *Biochim. Biophys. Acta 1230*, 74−76.
31. Moss, D. A., Nabedryk, E., Breton, J., and Mäntele, W. (1990) *Eur. J. Biochem. 187*, 565−572.
32. Baymann, F. (1995) Ph.D. Thesis, Fakultät für Biologie, Universität Freiburg, Germany.
33. Mäntele, W. (1996) in *Biophysical techniques in Photosynthesis* (Hoff, A. J., and Amesz, J., Eds.) Chapter 9, pp 137−160, Kluwer, Dordrecht.
34. Mäntele, W. (1993) *Trends Biochem. Sci. 18*, 197−202.
35. Yanisch-Perron, C., Vieira, J., and Messing, J. (1985) *Gene 33*, 103−119.
36. Herzberg, G. (1962) in *Molecular spectra and molecular structure: II. Infrared and Raman spectra of polyatomic molecules*, D. van Nostrand Company, Inc., Princeton, NJ.
37. Ostermeier, C., Harrenga, A., Ermler, U., and Michel, H. (1997) *Proc. Natl. Acad. Sci. U.S.A. 94*, 10547−10553.

BI9731697